


## Laser-induced structure transition of diamond-like carbon coated on cemented carbide and formation of reduced graphene oxide

**Abdelrahman Zkria** , Department of Applied Science for Electronics and Materials, Kyushu University, Kasuga, Fukuoka 816-8580, Japan; Department of Materials Science and Engineering, North Carolina State University, Raleigh, NC 27695-7907, USA; Department of Physics, Faculty of Science, Aswan University, Aswan 81528, Egypt

**Ariful Haque**, Department of Materials Science and Engineering, North Carolina State University, Raleigh, NC 27695-7907, USA

**Mohamed Egiza** and **Eslam Abubakr**, Department of Applied Science for Electronics and Materials, Kyushu University, Kasuga, Fukuoka 816-8580, Japan

**Koki Murasawa**, Department of Applied Science for Electronics and Materials, Kyushu University, Kasuga, Fukuoka 816-8580, Japan; OSG Corporation, 2-17 Shirakumo-cho, Toyokawa-shi, Aichi 442-0018, Japan

**Tsuyoshi Yoshitake**, Department of Applied Science for Electronics and Materials, Kyushu University, Kasuga, Fukuoka 816-8580, Japan

**Jagdish Narayan**, Department of Materials Science and Engineering, North Carolina State University, Raleigh, NC 27695-7907, USA

Address all correspondence to Abdelrahman Zkria at [abdelrahman\\_zkria@kyudai.jp](mailto:abdelrahman_zkria@kyudai.jp)

(Received 9 April 2019; accepted 20 June 2019)

### Abstract

We report on the structural evolution of diamond-like carbon (DLC) films by the nanosecond pulsed laser annealing process. DLC film is coated on cemented carbide (WC-Co) by cathodic arc ion plating, which is then annealed by ArF laser (193 nm, 20 ns) at different laser fluences (0.9–1.7 J/cm<sup>2</sup>). Upon laser annealing, Raman spectra divulge higher *sp*<sup>3</sup> fractions accompanied by a blue shift in the *G*-peak position, which indicates the changes of *sp*<sup>2</sup> sites from rings to chains. At higher fluence (>1.2 J/cm<sup>2</sup>), the film converts into reduced graphene oxide confirmed by its Raman-active vibrational modes: *D*, *G*, and 2*D*.

### Introduction

Carbon exists in several forms, including graphite, fullerenes, diamond-like carbon (DLC), diamond, nanotubes and graphene.<sup>[1]</sup> The ability of carbon to hybridize its bonds leads to a sensitive dependence of the properties of carbon materials on the *sp*<sup>2</sup> to *sp*<sup>3</sup> bonding ratio; consequently, they have emerged as potential materials for a wide range of applications. Amorphous DLC is a metastable carbon with a broad range of structures, comprised of carbon atoms of both *sp*<sup>2</sup> and *sp*<sup>3</sup> hybridizations arranged in a random network. Thus, the properties of DLC films could be a combination of those of graphite (purely *sp*<sup>2</sup> hybridized) and diamond (purely *sp*<sup>3</sup> hybridized) and depend on the fraction of *sp*<sup>3</sup> and *sp*<sup>2</sup> sites, the hydrogen content, and the ordering of *sp*<sup>2</sup> sites.<sup>[2,3]</sup> Owing to their unique properties, such as high hardness, smooth surface, low friction, chemical inertness, optical transparency, and high electrical resistivity, DLC films are becoming ideal for a variety of different industrial applications, including wear protective and anti-reflective coatings for tribological tools, biomedical coatings, magnetic storage media, and semiconductor devices.<sup>[4–8]</sup>

Diamond and DLC films are considered as ideal cutting tool coatings.<sup>[9]</sup> Although diamond has a higher hardness, DLC film can be obtained by simpler fabrication methods and, unlike diamond, it can be deposited at room temperature, which is an important practical advantage for coating applications. As a

candidate integration with DLC film, cemented carbide (WC-Co), comprising tungsten carbide and cobalt binder, is a practical material for cutting tools such as end mills and drill bits.<sup>[10,11]</sup> The DLC film coated on the WC-Co substrate is dense and smooth, unlike the rough surface of diamond film.<sup>[9]</sup> It is worth mentioning that the properties of these coatings depend mainly on the *sp*<sup>3</sup>/*sp*<sup>2</sup> ratio, which, in turn, depends on the method and conditions of the film's deposition. Conventionally, DLC films have been deposited from a hydrocarbon source gas, by plasma-enhanced chemical vapor deposition; and glow discharge deposition. Unintentionally, both methods produce films containing a significant proportion of hydrogen which leads to a loss of *sp*<sup>3</sup> bonding.<sup>[12]</sup> On the other hand, hydrogen-free DLC films can be formed using other physical vapor deposition methods employed pure carbon vapor, including laser ablation, arc evaporation, and magnetron sputtering of graphite targets.<sup>[13,14]</sup>

Post-treatment of DLC films has been studied for years, and particularly pulsed laser annealing (PLA) was widely applied to various materials, including amorphous Si,<sup>[15]</sup> graphene oxide,<sup>[16]</sup> diamond,<sup>[17]</sup> DLC films, and carbon nanotubes.<sup>[18,19]</sup> PLA (Nd:YAG laser,  $\lambda = 266$  nm) was demonstrated to achieve the crystallization of epitaxial oxide thin films with functional properties close to those reported for thermal treatments, but with shorter effective heating times.<sup>[20]</sup> In our most recent

work,<sup>[17]</sup> we proposed PLA (ArF laser,  $\lambda = 193$  nm) as a new potential method for shallow doping and the formation of conductive layers on single-crystalline diamond surfaces. Regarding DLC films, post UV-laser annealing was proposed to form high conductive transparent DLC structures.<sup>[21]</sup> Furthermore, Lee and Ki<sup>[22]</sup> demonstrated a laser-based method for rapidly fabricating graphene-based transparent conductive films on glass substrates by the laser annealing of DLC films in a shielding gas environment. Narayan's group experimentally demonstrated the conversion of amorphous carbon deposited onto low thermal conductivity substrates (sapphire) into Q-carbon (quenched carbon) and diamond nano- and microstructures by PLA, which show some extraordinary properties including excellent field emission characteristics and high temperature superconductivity.<sup>[23–25]</sup> In this process, the DLC films were melted rapidly in a super-undercooled state and subsequently quenched to room temperature within time  $< 200$  ns, wherein substrates with lower thermal conductivity trap heat flow, inducing larger undercooling, consequently, facilitating the formation of Q-carbon and diamond.<sup>[26]</sup> In this work, hydrogen-free DLC films were coated on WC-Co substrates through the cathodic arc ion plating method, and then the films were irradiated by ArF nanosecond pulsed laser (193 nm, 20 ns) at different laser energy densities (0.9–1.7 J/cm<sup>2</sup>). The composition and microstructure variations of the as-deposited (before PLA) and annealed films have been investigated by Raman spectroscopy and scanning electron microscopy.

## Experimental methods

### Film deposition and the nanosecond pulsed laser annealing process

Various deposition methods involve energetic species to deposit DLC films,<sup>[27,28]</sup> identifying the essential role of the particle energy in obtaining hard films with a significant  $sp^3$ -bonded carbon. In this study, the cathodic arc ion plating method was employed to deposit hydrogen-free DLC thin films onto WC-Co substrates. Cathodic arc ion plating is a high-energy deposition process that employs a vacuum arc to generate highly energetic ionized vapor from target materials. The substrate is negatively biased with respect to the anode, and the positive ions generated from the carbon target (purity of 99.99%) are deposited on the substrate. WC-Co (K-type cemented carbide,  $\phi 10 \times 5.5$  mm) with polished surface up to Ra = 0.003  $\mu\text{m}$  was used as the substrate. Before insertion of the substrates into the chamber, they were ultrasonically cleaned in acetone followed by methanol and then rinsed with deionized water. The films were deposited at a deposition rate of 0.3  $\mu\text{m}/\text{h}$  at a substrate temperature of less than 250 °C. To study the structural evolution of the deposited films, the Ultrafast nanosecond pulsed laser annealing (ns-PLA) process was operated by applying a single pulse of ArF excimer laser ( $\lambda = 193$  nm; full width at half maximum = 20 ns) at different energy densities of 0.9, 1.2, 1.5, and 1.7 J/cm<sup>2</sup>.

### Film characterizations: Raman spectroscopy and scanning electron microscopy

An essential requirement for studying carbon materials is the ability to identify all members of the carbon family using a powerful, nondestructive, fast, and high-resolution characterization tool. All these conditions are attainable by Raman spectroscopy, with the fact that most of the published papers on carbon materials have at least a Raman spectrum in them.<sup>[29]</sup> In our study, the quality of the carbonaceous structures before and after ns-PLA was investigated by micro-Raman spectroscopy. Raman spectra were obtained by using a confocal spectrometer/microscope (WITec confocal Raman microscope-alpha 3000 M) equipped with a thermodynamically cooled ( $-70$  °C) CCD camera and a microscope. The samples were illuminated with a continuous-wave diode-pumped solid-state laser providing 532 nm radiation. The 100 $\times$ /0.75 NA objective lens and a 3600 lines/mm grating were used to record the spectra. The accumulation time was 10 s, and the number of cycle during the accumulation was 10. The laser beam was focused on the sample to a spot of  $\sim 2$   $\mu\text{m}$  in diameter. The Raman scattering wavenumber axis was calibrated by a standard crystalline Si sample (characteristic Raman peak of Si (001) at 520.6  $\text{cm}^{-1}$ ). Parameters of the bands associated with the  $sp^2$ - and  $sp^3$ -bonded carbon were calculated by fitting the experimental spectra with Gaussian shape components. For phase identification, Raman measurements were correlated with high-resolution scanning electron microscopic (SEM) images acquired using the FEI Verios 460L field-emission scanning electron microscope.

## Results and discussion

Although the visible Raman spectroscopy is more sensitive to  $sp^2$  sites due to the excitation of their  $\pi$  states by visible photons, it is widely used for the characterization of DLC films to indirectly derive the  $sp^3$  fraction.<sup>[30]</sup> Visible Raman spectra of DLC/WC-Co films, before and after irradiation with a single laser pulse at different energy densities (0.9, 1.2, 1.5, and 1.7 J/cm<sup>2</sup>), are shown in Fig. 1. Non-irradiated (as-deposited) film shows a single peak due to the E2g phonon mode in the Brillouin zone center, which is commonly corresponding to the G-peak located in between 1500 and 1630  $\text{cm}^{-1}$ . This vibrational mode signifies bond stretching of  $sp^2$ -C atoms for both rings and chains.<sup>[31]</sup> The G-peak position in Fig. 1, located at 1525  $\text{cm}^{-1}$ , is in consistent with that (at 1526  $\text{cm}^{-1}$ ) of DLC film prepared by the mass selected C<sup>+</sup> ion beam deposition system reported by Praver et al.<sup>[32]</sup> Upon laser irradiation, an additional peak shoulder appears near 1340  $\text{cm}^{-1}$ , which represents the D-peak and can be attributed to A1g symmetry phonon near the K-zone boundary involving the breathing modes of  $sp^2$  carbon atoms.<sup>[29]</sup> For all the irradiated films, Raman spectra show distinct changes as a function of laser energy density, with the position of the G-peak shifting to higher values. The D-peak appears (which is practically absent in the as-deposited film), and its intensity rises with increasing laser energy density.

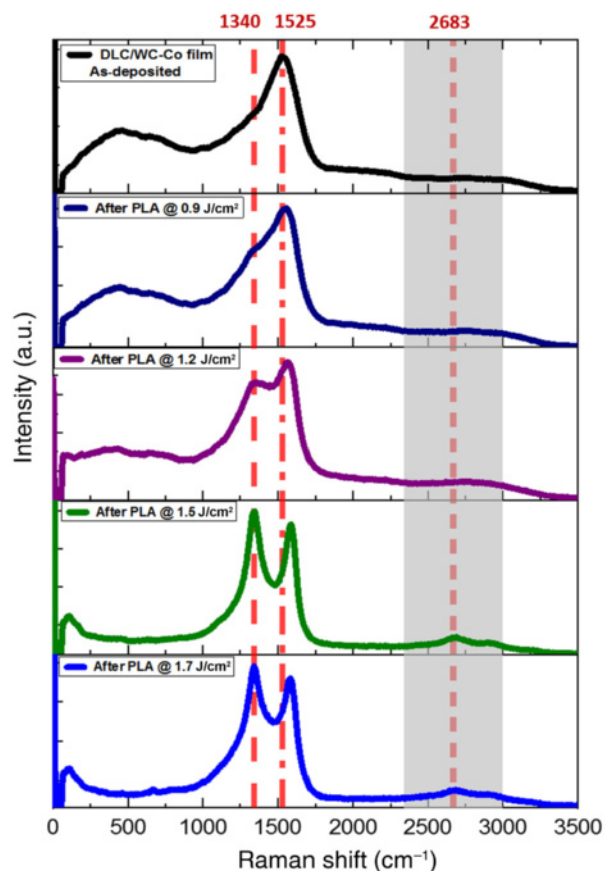


**Figure 1.** Typical visible Raman spectra of DLC/WC-Co film, as-deposited, and after ns-PLA at different pulsed laser energy densities over the range of 0–3500  $\text{cm}^{-1}$ .

It was reported<sup>[33]</sup> that the *G*-peak dispersion occurs only in more disordered carbon (no dispersion in graphite) due to the existence of different phonon modes. The dispersion arises from a resonant selection of  $sp^2$  configurations or clusters with wider  $\pi$ -band gaps and, correspondingly, higher vibration frequencies.<sup>[33]</sup> The appearance of *D*-peak and the rise of intensity with increasing laser energy is an indication of graphitization, since the *D*-peak is a well-known feature of the graphite spectrum.<sup>[34]</sup>

The mechanism of structural evolution of DLC/WC-Co films shown in Fig. 1 can be explained as follows: by ns-PLA, DLC films were melted and the atoms of the molten carbon (*metallic*) are closely packed. Followed by rapid quenching at room temperature, bonding characteristics change to covalent, which means the C–C-bonded tetrahedra are formed and packed randomly to form an amorphous structure. Resultant structure after annealing consists of  $sp^3$  bonding within the tetrahedra and a mixture of  $sp^3$  and  $sp^2$  between the tetrahedra. Here, the effect of laser annealing was different from the conversion of a-C film to Q-carbon that was reported by Narayan’s group.<sup>[23,35]</sup> The difference is mainly owing to

the employed deposition technique (KrF-PLD) and, consequently, properties of the evolving film, as well as the thermal conductivity of the substrate (sapphire). Both were confirmed to have a crucial effect in the formation of Q-carbon. Most recent experiments have shown that Cr-doping in sapphire renders a distinct transition from Q-carbon to  $sp^2$ -bonded films with increasing Cr content of sapphire. The higher content is expected to increase the thermal conductivity and undercooling.

To analyze the experimental data, three Gaussian peaks were used to accurately fit the acquired Raman spectra, with fixed peak positions at  $1140 \text{ cm}^{-1}$  (*T*-peak),  $1332 \text{ cm}^{-1}$  (*D*-peak), and  $1580 \text{ cm}^{-1}$  (*G*-peak), corresponding to Raman-active vibrational modes. Figures 2(a)–2(f) track the structural and morphological changes in DLC/WC-Co films, as-deposited, and after a single pulse of ArF laser at energy densities of 0.9 and 1.2  $\text{J}/\text{cm}^2$ , by Raman spectra and SEM micrograph. As shown in Fig. 2(a), reproduced fitted spectrum of as-deposited layer reveals *G*- and *D*-peaks at  $1547$  and  $1371 \text{ cm}^{-1}$ , respectively, C- $sp^{2\%}$  is calculated to be  $\sim 60\%$ , and rest is  $sp^3$ . The C- $sp^{2\%}$  decreased after laser annealing to 28% at 1.2  $\text{J}/\text{cm}^2$ , as shown in Fig. 2(c), and the *G*-peak has a blue shift with a value of  $30 \text{ cm}^{-1}$ . Based on the “three-stage model” proposed by Ferrari and Robertson,<sup>[29]</sup> visible Raman spectra for all disordered carbons can be classified into three stages: (1) perfect graphite to nanocrystalline graphite, (2) nanocrystalline graphite to  $sp^2$  amorphous carbon, and (3)  $sp^2$  amorphous carbon to  $sp^3$  tetrahedral amorphous carbon. Results of our films follow the trend of disordering of amorphous carbon in stage 3, with the main changes of increasing  $sp^3$  content accompanied by the blue shift of *G*-peak by laser annealing. This behavior is attributed to the changes of  $sp^2$  sites from rings to chains, specifically from delocalized aromatic bonds to the shorter localized olefinic bonds (C=C), which have higher vibration frequencies.<sup>[36]</sup>

In agreement with Raman spectra, the transformation of DLC films after ns-PLA is visually observed in the SEM images, shown in Figs. 2(d)–2(f). SEM image depicts the smooth surface of non-irradiated (before PLA) film at low and high resolutions. While after PLA, the morphology of the films is drastically changed to show the formation of the clusters. All DLC films homogeneously covered the WC-Co substrates, without peeling off or delamination, even after the PLA.

Raman spectrum of irradiated films at 1.7  $\text{J}/\text{cm}^2$  together with fitting results are shown in Fig. 3. The spectrum exhibited intense *D*- and *G*-peaks, *2D* peak, and in the inset (upper left side), SEM image shows the dense cluster formation. Commonly, *2D* vibrational mode centered at  $2698 \text{ cm}^{-1}$  is the second-order overtone of the *D*-peak, it is the characteristic of double-resonance transitions resulting from the generation of two phonons with opposite momentum ( $+k$  and  $-k$ ) to each other.<sup>[37]</sup> The *2D* band ( $2683 \text{ cm}^{-1}$ ) appearing in the spectra corresponds to the reduced-graphene oxide (rGO) structures formed after annealing at higher laser energy. The inset of Fig. 3 is showing peak fittings of the *2D* vibrational mode.

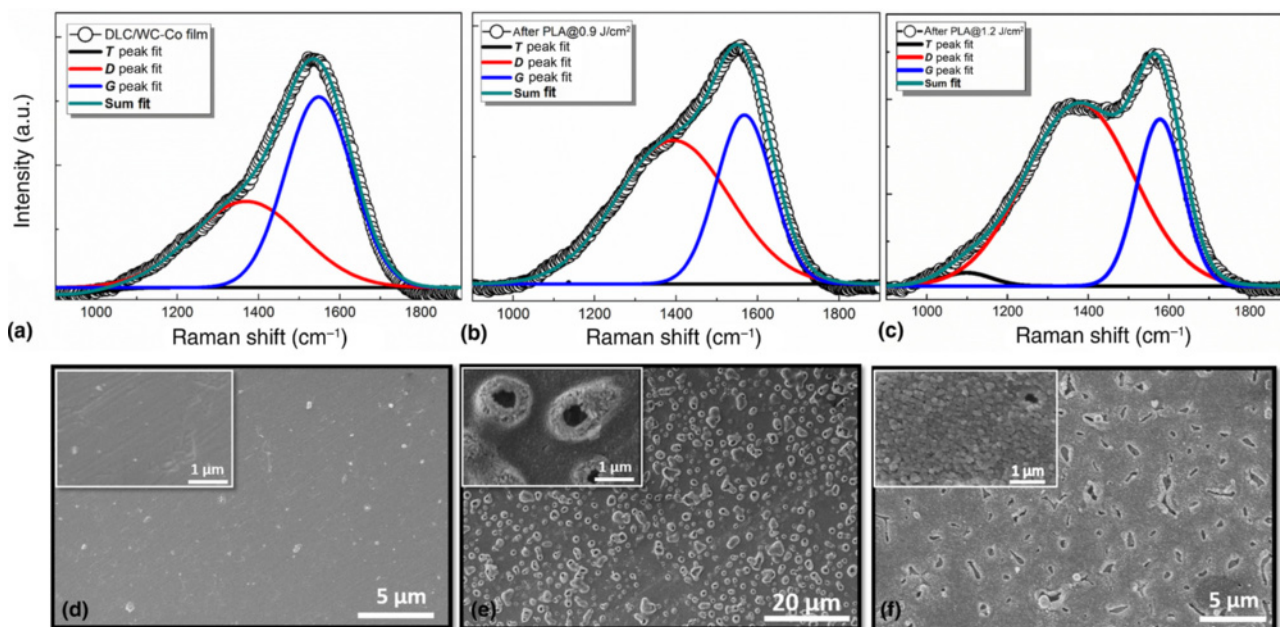


**Figure 2.** Raman spectra and SEM images: (a),(d) as-deposited and after ns-PLA processed at (b),(e) 0.9 J/cm<sup>2</sup> and (c),(f) 1.2 J/cm<sup>2</sup>.

It has four components, namely  $2D_{1B}$ ,  $2D_{1A}$ ,  $2D_{2A}$ ,  $2D_{2B}$ , which indicate the formation of two layers of rGO, in consistent with the Raman spectrum of graphene layers reported by Ferrari et al.<sup>[38]</sup>

In the rGO thin films, there are several parameters which contribute to the structural and electrical characteristics. Among them, the average size ( $L_D$ ) of  $sp^2$  clusters and the defect density in the 2D system play crucial roles.<sup>[39]</sup> The earlier studies on the rGO films used the  $I_D/I_G$  ratio as an important parameter to calculate the average size ( $L_D$ ) of  $sp^2$  clusters in

the rGO structure.<sup>[38]</sup> The following equation is ideally used to calculate the  $L_D$ :

$$L_D^2(\text{nm}^2) = (1.8 \times 10^{-9}) \lambda_L^4 \left( \frac{I_D}{I_G} \right)^{-1} \quad (1)$$

where  $\lambda_L$  is the wavelength in nm (532.06 nm) of the excitation source for Raman spectroscopy. The same parameter ( $I_D/I_G$ ) can also be used to calculate the defect density,  $n_D(\text{cm}^{-2})$ , in the 2D system by using the following equation<sup>[40]</sup>:

$$n_D(\text{cm}^{-2}) = \left( \frac{1.8 \times 10^{22}}{\lambda_L^4} \right) \left( \frac{I_D}{I_G} \right) \quad (2)$$

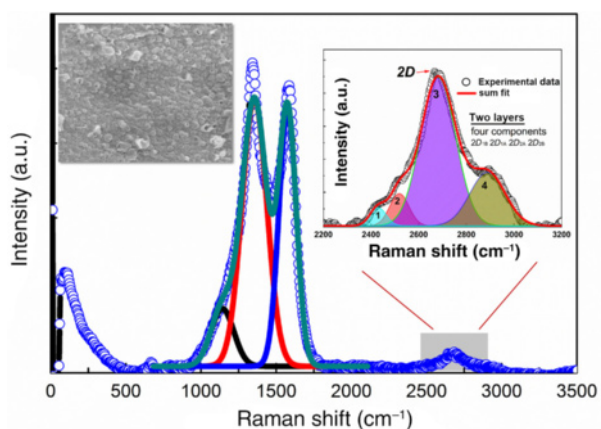


**Figure 3.** Raman spectrum of DLC/WC-Co film after ns-PLA processed at higher energy density of 1.7 J/cm<sup>2</sup>. Insets are SEM image and fitting of 2D-peak.

For PLA (at 1.7 J/cm<sup>2</sup>)-grown rGO film, the values of the average size of the  $sp^2$  domains and defect density are calculated to be 9.81 nm and  $3.37 \times 10^{11}$ , respectively. These values are in consistent with those reported previously for rGO films.<sup>[40,41]</sup> Therefore, the cathodic arc ion plating deposition of DLC and the successive ns-PLA process of the DLC at a higher energy density render high-quality device grade rGO films.

The shift in the  $G$ - and  $D$ -peaks and the  $D$ -peak intensity in Raman spectra of DLC films can provide important information about the film structure, especially related to  $sp^2$  and  $sp^3$  fractions.<sup>[42]</sup> Figure 4 shows the variation of  $G$ -peak positions and the  $sp^3/sp^2$  ratio (in the inset) as a function of laser energy densities. It is observed that the as-deposited film with low  $sp^3$  fraction (40%) has a low  $G$ -band frequency of  $1547 \text{ cm}^{-1}$ , whereas the film (annealed at 1.2 J/cm<sup>2</sup>) with a high  $sp^3$  fraction (73%)

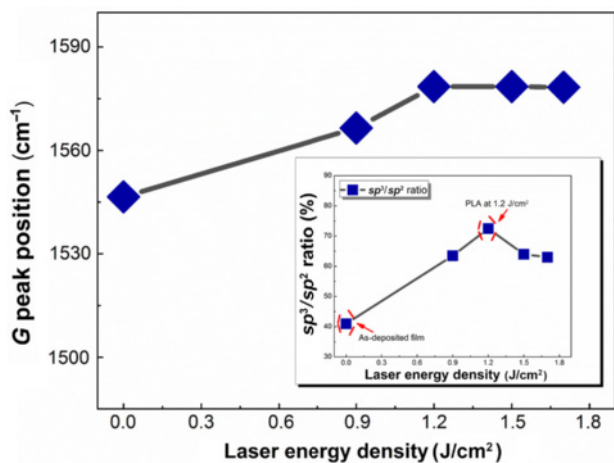


**Figure 4.** The variations of *G*-peak positions with different laser energy densities extracted from the fitting of acquired Raman spectra. Inset is the  $sp^3/sp^2$  ratio.

has a high frequency of about  $1578\text{ cm}^{-1}$ . These results are in coincidence with the non-hydrogenated amorphous film reported by Anders et al.<sup>[34]</sup> On the other hand, increasing laser energy density ( $>1.2\text{ J/cm}^2$ ) exhibited a decreased  $sp^3$  fraction without any shift in the *G*-band frequency. Generally, the  $sp^2$  configuration varies consistently with the  $sp^2$  fraction. However, Ferrari and Robertson<sup>[29]</sup> reported that the  $sp^2$  configuration can be changed independently from the  $sp^2/sp^3$  ratio called “hysteresis phenomenon.” This phenomenon typically occurs for films those annealed after deposition, which is applicable to our study on DLC/WC-Co films.

## Conclusions

This article provides a study of systematic changes in the structure of DLC thin films with a controlled variation in the laser energy density during the PLA process. Hydrogen-free DLC films with the  $sp^3$  content of 40% are deposited on WC-Co substrates using the cathodic arc ion plating method. Nanosecond laser melting and subsequent quenching of the films, as a highly non-equilibrium process, lead to phase transformation of DLC into rGO. High-resolution SEM images visualize the drastic changes in the film morphology from the smooth as-deposited film (before PLA) to the formation of clusters after PLA. Raman investigation of irradiated films shows a blue shift of the *G*-band frequency accompanied with an increase in  $sp^3$  fraction. At a higher laser energy density, Raman spectrum indicates the presence of *D*, *G*, and 2*D* Raman-active vibrational modes and characteristics of rGO thin films. Two important structural parameters, i.e., the domain size of  $sp^2$  clusters and defect density, of the PLA-grown rGO were also calculated using the parameters extracted from the Raman fitting profiles. Overall, this study on the structural evolution of the laser-annealed DLC and the formation of rGO on the WC-Co substrate have profound

scientific importance in the development of nanomaterials coupling WC/rGO as a high-efficient, low-cost electrocatalyst for the hydrogen evolution reaction.

## Supplementary material

The supplementary material for this article can be found at <https://doi.org/10.1557/mrc.2019.88>.

## Acknowledgments

This work was supported by the Japan Society for the Promotion of Science (JSPS KAKENHI Grant No. JP15H04127) and Grant-in-Aid for JSPS Fellows (Grant No. JP17F17380). A. Zkria acknowledges Japan Society for Promotion of Science (JSPS), Japan for awarding the JSPS fellowship and supporting visit at North Carolina State University as a visiting scientist. For sample characterizations, we used the Analytical Instrumentation Facility (AIF) at North Carolina State University, which is supported by the State of North Carolina.

## References

- H.O. Pierson: *Handbook of Carbon, Graphite, Diamonds and Fullerenes: Processing, Properties and Applications* (William Andrew, Noyes Publications, Park Ridge, New Jersey, USA, 2012).
- J. Robertson: Hard amorphous (diamond-like) carbons. *Prog. Solid State Chem.* **21**, 199 (1991).
- A. Zkria, F. Abdel-Wahab, Y. Katamune, and T. Yoshitake: Optical and structural characterization of ultrananocrystalline diamond/hydrogenated amorphous carbon composite films deposited via coaxial arc plasma. *Curr. Appl. Phys.* **19**, 143–148 (2019).
- S.R.P. Silva, J. Robertson, W.I. Milne, and G.A.J. Amarutunga: *Amorphous Carbon: State of the Art* (World Scientific, Singapore, 1998).
- C. Casiraghi, J. Robertson, and A.C. Ferrari: Diamond-like carbon for data and beer storage. *Mater. Today* **10**, 42 (2007).
- R. Hauert: An overview on the tribological behavior of diamond-like carbon in technical and medical applications. *Tribol. Int.* **37**, 991 (2004).
- M. Milewski, M. Madej, M. Niemczewska-Wójcik, and D. Ozimina: Evaluation of the properties of diamond-like carbon coatings lubricated with ionic liquids. *Tribologia* **5**, 37–45 (2017).
- J. Kowalczyk, M. Milewski, M. Madej, and D. Ozimina: Properties of a tribological system with a diamond-like carbon coating lubricated with environmentally friendly cutting fluid. *Tribologia* **5**, 19–26 (2018).
- M. Dai, K. Zhou, Z. Yuan, Q. Ding, and Z. Fu: The cutting performance of diamond and DLC-coated cutting tools. *Diam. Relat. Mater.* **9**, 1753–1757 (2000).
- A. Saai, I.H. Svenum, P.A. Kane, J. Friis, and T. Berstad: Multi-scale modeling of WC-Co drill bits material with density functional theory and crystal elasticity model. *Proc. Mater. Sci.* **3**, 640 (2014).
- H. Naragino, M. Egiza, A. Tominaga, K. Murasawa, H. Gonda, M. Sakurai, and T. Yoshitake: Hard coating of ultrananocrystalline diamond/nonhydrogenated amorphous carbon composite films on cemented tungsten carbide by coaxial arc plasma deposition. *Appl. Phys. A* **122**(8) (2016).
- Z.L. Akkerman, H. Efstathiadis, and F.W. Smith: Thermal stability of diamond like carbon films. *J. Appl. Phys.* **80**, 3068 (1996).
- E. Manikandan, G. Kavitha, and J. Kennedy: Epitaxial zinc oxide, graphene oxide composite thin-films by laser technique for micro-Raman and enhanced field emission study. *Ceram. Int.* **40**(10), 16065 (2014).
- E. Manikandan, J. Kennedy, G. Kavitha, K. Kaviyarasu, M. Maaza, B.K. Panigrahi, and U.K. Mudali: Hybrid nanostructured thin-films by PLD for enhanced field emission performance for radiation micro-nano dosimetry applications. *J. Alloys Compd.* **647**, 141 (2015).

- 15 S.G. Ryu, I. Gruber, C.P. Grigoropoulos, D. Poulidakos, and S.J. Moon: Large area crystallization of amorphous Si with overlapping high repetition rate laser pulses. *Thin Solid Films* **520**(22), 6724 (2012).
- 16 R. Trusovas, G. Račiukaitis, G. Niaura, J. Barkauskas, G. Valušis, and R. Pauliukaite: Recent advances in laser utilization in the chemical modification of graphene oxide and its applications. *Adv. Opt. Mater.* **4**(1), 37–65 (2016).
- 17 E. Abubakr, A. Zkria, Y. Katamune, S. Ohmagari, K. Imokawa, H. Ikenoue, and T. Yoshitake: Formation of low resistivity layers on singlecrystalline diamond immersed in boric acid by excimer laser irradiation. *Diam. Relat. Mater.* **95**, 166 (2019).
- 18 J. Narayan, V. Godbole, and C. White: Laser method for synthesis and processing of continuous diamond films on nondiamond substrates. *Science* **252**, 416 (1991).
- 19 J. Narayan, A. Bhaumik, R. Sachan, A. Haque, S. Gupta, and P. Pant: Direct conversion of carbon nanofibers and nanotubes into diamond nanofibers and the subsequent growth of large-sized diamonds. *Nanoscale* **115**, 2238–2248 (2019).
- 20 A. Queraltó, A. Pérez del Pino, M. de la Mata, J. Arbiol, M. Tristany, X. Obradors, and T. Puig: Ultrafast epitaxial growth kinetics in functional oxide thin films grown by pulsed laser annealing of chemical solutions. *Chem. Mater.* **28**(17), 6136 (2016).
- 21 F. Stock, F. Antoni, L. Diebold, C.C. Gowda, S. Hajjar-Garreau, D. Aubel, and D. Muller: UV laser annealing of diamond-like carbon layers obtained by pulsed laser deposition for optical and photovoltaic applications. *Appl. Surface Sci.* **464**, 562–566 (2019).
- 22 K. Lee and H. Ki: Rapid fabrication of transparent conductive films with controllable sheet resistance on glass substrates by laser annealing of diamond-like carbon films. *Acta Mater.* **111**, 315–320 (2016).
- 23 J. Narayan, A. Bhaumik, S. Gupta, A. Haque, and R. Sachan: Progress in Q-carbon and related materials with extraordinary properties. *Mater. Res. Lett* **6**(7), 353–364 (2018).
- 24 A. Haque and J. Narayan: Stability of electron field emission in Q-carbon. *MRS Commun* **8**(3), 1343–1351 (2018).
- 25 A. Bhaumik, R. Sachan, S. Gupta, and J. Narayan: Discovery of high-temperature superconductivity ( $T_c=55$  K) in B-doped Q-carbon. *ACS Nano* **11**(12), 11915–11922 (2017).
- 26 S. Gupta, R. Sachan, A. Bhaumik, P. Pant, and J. Narayan: Undercooling driven growth of Q-carbon, diamond, and graphite. *MRS Commun* **8**, 533–540 (2018).
- 27 Y. Lifshitz: Hydrogen-free amorphous carbon films: correlation between growth conditions and properties. *Diam. Relat. Mater* **5**, 388–400 (1996).
- 28 A. Zkria, H. Gima, M. Shaban, and T. Yoshitake: Electrical characteristics of nitrogen-doped ultrananocrystalline diamond/hydrogenated amorphous carbon composite films prepared by coaxial arc plasma deposition. *Appl. Phys. Express* **8**, 095101-1–095101-3 (2015).
- 29 A.C. Ferrari and J. Robertson: Interpretation of Raman spectra of disordered and amorphous carbon. *Phys. Rev. B* **61**, 14095 (2000).
- 30 S.R. Salis, D.J. Gardiner, M. Bowden, J. Savage, and D. Rodway: Monitoring the quality of diamond films using Raman spectra excited at 514.5 nm and 633 nm. *Diam. Relat. Mater.* **5**, 589 (1996).
- 31 J. Yan, Y. Zhang, P. Kim, and A. Pinczuk: Electric field effect tuning of electron-phonon coupling in graphene. *Phys. Rev. Lett.* **98**, 166802 (2007).
- 32 S. Praver, K.W. Nugent, Y. Lifshitz, G.D. Lempert, E. Grossman, J. Kulik, I. Avigal, and R. Kalish: Systematic variation of the Raman spectra of DLC films as a function of sp<sup>2</sup>:sp<sup>3</sup> composition. *Diam. Relat. Mater.* **5**, 433 (1996).
- 33 A.C. Ferrari: Determination of bonding in diamond-like carbon by Raman spectroscopy. *Diam. Relat. Mater* **11**, 1053–1061 (2002).
- 34 S. Anders, J.W. Ager III, G.M. Pharr, T.Y. Tsui, and I.G. Brown: Heat treatment of cathodic arc deposited amorphous hard carbon films. *Thin Solid Films* **308**, 186–190 (1997).
- 35 J. Narayan and A. Bhaumik: Q-carbon discovery and formation of single-crystal diamond nano- and microneedles and thin films. *Mater. Res. Lett* **4**, 118–126 (2016).
- 36 D. Lin-Vien, N.B. Colthrup, W.G. Fateley, and J.G. Grasselli: *The Handbook of Infrared and Raman Characteristic Frequencies of Organic Molecules* (Academic, New York, 1991).
- 37 S. Piscanec, M. Lazzeri, F. Mauri, A.C. Ferrari, and J. Robertson: Kohn anomalies and electron-phonon interactions in graphite. *Phys. Rev. Lett* **93**(18), 185503-1–185503-4 (2004).
- 38 A. Ferrari, J. Meyer, V. Scardaci, C. Casiraghi, M. Lazzeri, F. Mauri, S. Piscanec, D. Jiang, K. Novoselov, S. Roth, and A.K. Geim: Raman Spectrum of Graphene and Graphene Layers. *Phys. Rev. Lett.* **97**, 187401 (2006).
- 39 A. Haque, M. Abdullah-Al Mamun, M.F.N. Taufique, P. Karnati, and K. Ghosh: Temperature dependent electrical transport properties of high carrier mobility reduced graphene oxide thin film devices. *IEEE Trans. Semicond. Manuf* **31**(4), 535–544 (2018).
- 40 H. Xu, Z. Zhang, R. Shi, H. Liu, Z. Wang, S. Wang, and L.-M. Peng: Batch-fabricated high-performance graphene Hall elements. *Sci. Rep* **3**, 1207-1–1207-8 (2013).
- 41 A. Bhaumik, A. Haque, M.F.N. Taufique, P. Karnati, R. Patel, M. Nath, and K. Ghosh: Reduced graphene oxide thin films with very large charge carrier mobility using pulsed laser deposition. *J. Mater. Sci. Eng* **6**(4), 364-1–364-11 (2017).
- 42 M.A. Tamor and W.C. Vassell: Raman ‘fingerprinting’ of amorphous carbon films. *J. Appl. Phys* **76**(6), 3823–3830 (1994).